J Occup Health 2011; 53: 64–74

Journal of Occupational Health

Evaluation of Acute Oxidative Stress Induced by NiO Nanoparticles *In Vivo* and *In Vitro*

Masanori HORIE[1], Hiroko FUKUI[1], Keiko NISHIO[1], Shigehisa ENDOH[2], Haruhisa KATO[3], Katsuhide FUJITA[4], Arisa MIYAUCHI[2], Ayako NAKAMURA[3], Mototada SHICHIRI[1], Noriko ISHIDA[1], Shinichi KINUGASA[3], Yasuo MORIMOTO[5], Etsuo NIKI[1], Yasukazu YOSHIDA[1] and Hitoshi IWAHASHI[1]

[1]Health Research Institute, [2]Research Institute for Environmental Management Technology, [3] National Metrology Institute of Japan, [4] Research Institute of Science for Safety and Sustainability, National Institute of Advanced Industrial Science and Technology and [5]Institute of Industrial Ecological Sciences, University of Occupational and Environmental Health, Japan

Abstract: Evaluation of Acute Oxidative Stress Induced by NiO Nanoparticles *In Vivo* and *In Vitro*: Masanori HORIE, *et al*. Health Research Institute —Objectives: Nickel oxide (NiO) is an important industrial material, and it is also a harmful agent. The toxicity of NiO is size-related: nanoparticles are more toxic than fine-particles. The toxic mechanism induced by NiO nanoparticles remains unexplained, and the relationship between *in vitro* and *in vivo* NiO toxicity results is unclear. In the present study, we focused on the oxidative stress caused by NiO nanoparticles by examining and comparing *in vitro* and *in vivo* acute responses induced by NiO nanoparticles. **Methods:** Cellular responses induced by black NiO nanoparticles with a primary particle size of 20 nm, were examined in human lung carcinoma A549 cells. *In vivo* responses were examined by instillation of NiO nanoparticles into rat trachea. Bronchoalveolar lavage fluid (BALF) was collected after intratracheal instillation at different time points, and concentrations of lipid peroxide heme oxygenase-1 (HO-1), surfactant protein-D (SP-D) and lactate dehydrogenase (LDH) in BALF were measured. **Results:** The levels of intracellular reactive oxygen species and lipid peroxidation in A549 cells increased with increasing exposure to NiO nanoparticles, and increases in gene expressions of HO-1 and SP-D were observed in A549 cells. The lipid peroxide level in BALF significantly increased after 24 h instillation but decreased three days later. LDH leakage was also observed three days later. **Conclusions:** NiO nanoparticles induce oxidative stress-related lung injury. *In vivo* and *in vitro* oxidative stress was induced resulting in activation of antioxidant systems. Based on these responses, we conclude that the results of the *in vivo* and *in vitro* studies tend to correspond.
(J Occup Health 2011; 53: 64–74)

Key words: BALF, Culture cell, Cytotoxicity, Nanoparticle, Nickel oxide, Oxidative stress

Nickel oxide (NiO) is an important material used for electronic components, catalysts and ceramic materials. It is also known that nickel compounds (including NiO) have harmful effects. Nickel compounds are classified as class 1 carcinogenic material by the International Agency for Research on Cancer (IARC Monographs on the Evaluation of Carcinogenic Risks to Humans, Volume 49, 1990). In general, NiO is classified as having relatively lower toxicity than other nickel compounds[1, 2]. The main cause of nickel toxicity is the nickel ion, so the solubility of nickel compounds is an important factor in their toxicities. For example, the solubility of NiO is lower than that of nickel subsulfide (Ni_3S_2) and the toxicity of NiO is lower than that of Ni_3S_2[3]. In regard to particle size, NiO nanoparticles have a higher solubility than fine particles[4]. NiO nanoparticles release more Ni^{2+} per weight than fine particles; thus, the toxicity of nanoparticles is greater than that of fine particles. Also, *in vitro* examinations have revealed that cellular uptake of NiO nanoparticles allows release of Ni^{2+} within the cell[4]. Namely, the cytotoxicity of NiO nanoparticles is caused by dissolution of the particles inside cells. In addition,

Received Aug 18, 2010; Accepted Nov 18, 2010
Published online in J-STAGE Jan 11, 2011
Correspondence to: M. Horie, Health Research Institute, AIST, 1-8-31 Midorigaoka, Ikeda, Osaka 563-8577, Japan
(e-mail: masa-horie@aist.go.jp)

NiO nanoparticles induce stronger oxidative stress than fine-particles[5].

Oxidative stress is an important factor for the risk assessment of NiO nanoparticles[6]. It is also a factor involved in health and disease: aging, neurological disorders (e.g., Alzheimer's disease, Parkinson's disease)[7], diabetes and arteriosclerosis[8]. It has been reported that oxidative stress is also linked to carcinogenesis due to gene alteration[9]. In many carcinogenesis models, the level of major modified base produced by oxidative stress, 8-OHdG[10, 11], increases in target organs[12]. Hydrogen peroxide (H_2O_2) is a strong oxidant produced chemically and enzymatically *in vivo* and reacts with metals to produce reactive species such as hydroxyl radicals, and metal–hydroperoxo complexes which injure DNA by oxidation[13, 14]. DNA is also injured by peroxy radicals and singlet oxygens[15].

In an organism exposed to oxidative stress, lipids, nucleic acids and proteins are attacked and the oxide molecules described above are produced[16]. Simultaneously, anti-oxidative responses such as production of glutathione and expression of heme oxygenase-1 (HO-1) are activated[17, 18]. Inhalation of asbestos and crystalline silica induce severe oxidative stress and subsequent expression of HO-1[19, 20]. Detection of the level of oxidative stress is an important factor in forecasting a disease. If oxidative stress is weak and acute, there is a decrease in the production of biomolecules. On the other hand, persistent and strong oxidative stress causes sickness due to failure of the defense system[21].

Among biomolecules, highly unsaturated fatty acids are readily oxidized[22]. Lipid peroxide (LOOH) is produced by the reaction of an unsaturated fatty acid with reactive oxygen species (ROS). *In vivo*, polyunsaturated fatty acids such as linoleic acid and arachidonic acid preferentially undergo hydroperoxidation[23]. Linoleic acid is an abundant lipid *in vivo* and its free radical-mediated oxidation produces hydroperoxy octadecadienoate (HPODE) as the primary product. Yoshida and Niki proposed the measurement of total hydroxyoctadecanoic acid (tHODE) as a biomarker of oxidative stress *in vivo*[24]. Hydroperoxides and ketones as well as hydroxides of both free and ester forms of linoleic acid are measured as tHODE. The level of tHODE is related to various diseases[25–28]. Carbon tetrachloride, which is a strong inducer of free radicals, induced a drastic increase in the level tHODE in rodent livers[29]. Also, lipid peroxidation was observed in cells exposed to metal oxide nanoparticles[30].

In vivo inhalation of NiO induced severe toxic effects such as inflammation and collagen deposition in the lung[31–33]. Although some investigations of the toxic effect of nanoparticles *in vivo* have been performed[34, 35], details of biological responses induced by NiO nanoparticles are still unclear. *In vitro* examinations are important and essential for clarification of toxic mechanisms. However, the relationship between *in vitro* and *in vivo* examinations is also unclear. In general, nanoparticles have higher physical and chemical activity than fine particles because of their higher surface area per weight. The industrial advantages and increase in usage of nanoparticles also means an increase in potential biological effects and toxic risks.

In this study, we examined the biological responses induced by exposure to NiO nanoparticles *in vivo* and *in vitro*, focusing particularly on the biological response of oxidative stress.

Materials and Methods

Cell culture

Human lung carcinoma A549 cells were purchased from the Riken BioResource Center (Tsukuba, Ibaraki, Japan). Cells were cultured in Dulbecco's modified Eagle medium (DMEM; Gibco, Invitrogen Corporation, Grand Island, NY) and supplemented with 10% heat-inactivated fetal bovine serum (FBS; CELLect GOLD; MP Biomedicals Incorporated, Solon, OH), 100 units/m*l* of penicillin, 100 μg/m*l* of streptomycin, and 250 ng/m*l* of amphotericin B (Nacalai Tesque Incorporated, Kyoto, Japan). In the present study, this DMEM cocktail is called "DMEM-FBS".

Cells were cultured in DMEM-FBS and incubated at 37°C, under 5% CO_2 in air. For cellular experiments, cells were seeded at 2×10^5 cells/m*l* in 6-well multidishes (Corning Incorporated, Corning, NY) and incubated for 24 h. Then the medium was changed to a NiO dispersion, and incubated for another 24 h.

In some experiments, the cells were pre-treated with α-tocotrienol (Eisai Co., Ltd. Tokyo, Japan) and N-acetylcysteine (NAC; Sigma-Aldrich, St. Louis, MO). The cells were seeded at 1×10^5 cells/m*l* and incubated for 24 h. Subsequently, the medium was changed to fresh medium containing 5 μM α-tocotrienol and 2 mM NAC and incubated for another 24 h. Then, the medium was removed, and exposed to the NiO dispersion containing 5 μM α-tocotrienol and 2 mM NAC and incubated for another 24 h.

Nickel oxide particles and preparation of NiO dispersion

NiO (black) nanoparticles were purchased from Nanostructured and Amorphous Materials, Inc. (Houston, TX). According to the manufacturer's data sheet, the primary particle size and specific surface area were 20 nm and 50–80 m^2/g, respectively. $NiCl_2$ was purchased from Wako Pure Chemical Industries, Limited (Osaka, Japan).

For cellular experiments, a stable and uniform NiO culture medium dispersion was prepared by pre-adsorption and centrifugation as previously described[36]. To prevent cell starvation due to adsorption of medium components

onto the surface of NiO nanoparticles, NiO nanoparticles were pre-treated with FBS (80 mg/m*l*). Then, the secondary particle sizes were adjusted by centrifugation.

For animal experiments, 1 g of NiO powder was dispersed in 200 m*l* of endotoxin-free distilled water. NiO particles were dispersed by ultrasonication for 10 min; then, the dispersion was cooled for 10 min on ice. Ultrasonication and cooling were repeated nine times. The particle size was adjusted by centrifugation at 10,000 × g for 20 min and filtration with a 1-mm membrane filter. The NiO concentration was adjusted with distilled water. Endotoxin activities in the dispersion and distilled water were negative as detected by the Limulus Amebocyte Lysate Assay (Pyrotell: Associates of Cape Cod, Incorporated, East Falmouth, MA). The concentration of NiO in the dispersion was measured in the solid mass measuring after drying the dispersion at 200°C for 3 h. The size distribution of NiO particles in the dispersion was measured by dynamic light scattering (DLS) using a Zetasizer Nano machine (Malvern Instruments Limited, Malvern, United Kingdom).

The Ni^{2+} concentrations in NiO dispersions were determined by colorimetry using 2-(5-bromo-2-pyridylazo)-5-[*N*-*n*-propyl-*N*-(3-sulfopropyl)amino] aniline (5-Br-PSAA) (Dojindo Laboratories, Kumamoto, Japan), in accordance with the procedure outlined by Ohno *et al*.[37]. NiO dispersions or cell culture supernatants were centrifuged at 16,000 ×g for 20 min, and the supernatant was carefully collected. After suitable dilution of the supernatant, 50 μl of supernatant and 50 μl of 1 mM 5-Br-PSAA were added to 2.9 m*l* of buffer solution (60 mM KH_2PO_4, 20 mM $Na_2B_4O_7$ $10H_2O$, 0.2% Tiron, pH 6.9). The solution was mixed well, and its absorbance at 568 nm was measured using a DU530-spectrophotometer (Beckman Coulter Inc., Miami, FL). The Ni^{2+} concentration was estimated from the standard curve for nickel standard solutions (Wako Pure Chemical Industries).

Characterization of the NiO-DMEM-FBS dispersion for in vitro examinations

The NiO-DMEM-FBS dispersion prepared by the method described above was divided into three parts that were used for simultaneous biological experiments, nickel-concentration measurements, and particle-size measurements. The secondary particle size of the NiO-DMEM-FBS dispersion was measured by DLS in the same way as described previously[38]. The total nickel concentration was measured by X-ray fluorescence analysis (XRF). Thirteen milliliters of metal oxide-DMEM-FBS dispersion were added to 13 m*l* of standard solution including 0.1 mg/m*l* of Fe as an internal standard element and mixed well. Five milliliters of the mixture were dried in an oven at 200°C for 24 h. The dried sample was ground in an agate mortar and XRF was performed using an energy dispersive X-ray fluorescence spectrometer JSX-3201 (Jeol Limited, Tokyo, Japan). The amount of nickel was estimated from the molar ratio of nickel and the internal standard. The concentration of soluble nickel was measured by inductively coupled plasma mass spectrometry (ICP- AES) (ICP; SPS 4000, Seiko Instruments Inc., Chiba, Japan) with ultrafiltration. To completely remove the particulate nickel, the dispersion was allowed to stand for 24 h. Then, 10 m*l* of the dispersion was applied to the ultrafiltration membrane (molecular weight cutoff was 50,000: Vivaspin 20–50k, GE Healthcare UK Limited, Buckinghamshire, United Kingdom) and centrifuged at 6,000 × g for 60 min. The membrane was washed thrice with 5 m*l* of Milli-Q water, and the amount of nickel in the filtrate was measured by ICP-AES.

Measurement of intracellular oxidative stress

Intracellular ROS were detected using 2',7'-dichlorofluorescin diacetate (DCFH-DA; Sigma–Aldrich, St. Louis, MO). DCFH-DA was dissolved in dimethyl sulfoxide (DMSO) at 5 mM as a stock solution and stored at –20°C. When used in an experiment, it was diluted 500 times with serum-free medium. After exposure of the cells to NiO dispersion for 24 h, the medium was changed to serum-free DMEM that included 10 μM of DCFH-DA and incubated for 30 min at 37°C. Cells were then washed once with PBS, collected by 0.25% trypsinization, washed once with PBS, and resuspended in 500 μl of PBS. Cell samples in PBS were excited with a 488-nm argon ion laser in a Cytomics FC500 flow cytometry system (Beckman Coulter, Inc., Brea, CA), and the emission of 2',7'-dichlorofluorescein (DCF) was measured at 525 nm. Data were collected from at least 5,000 gated events.

Intracellular hydroperoxide was detected using diphenyl-1-pyrenylphosphine (DPPP; Dojindo Laboratories, Kumamoto, Japan). DPPP was dissolved in DMSO at 5 mM as a stock solution and stored at –20°C. When used in an experiment, it was diluted 100-times with serum-free medium. After exposure of the cells to NiO dispersion for 24 h, the medium was changed to serum-free DMEM that included 50 μM of DPPP and incubated for 30 min at 37°C. Cells were then washed once with PBS, harvested by trypsinization, washed once with PBS, and resuspended in 3 m*l* of PBS. Cell samples in PBS were excited with a 351-nm argon ion laser and the emission of DPPP oxide was measured at 380 nm using an RF-5300PC spectrofluorophotometer (Shimadzu Corporation, Kyoto, Japan). After measurement, the cells were collected and measured for protein concentration. DPPP oxide fluorescence was compensated for by cellular protein concentration.

Analyses of tHODE were carried out according to the method of Yoshida *et al*.[39], with some modification using liquid chromatography coupled to quadrupole mass

spectrometry (LC–MS/MS). tHODE includes free and ester forms of hydroperoxides and ketones as well as hydroxides of linoleic acid. For internal standards, 13-S-hydroxy-10E, 12Z-octadecadienoic-9, 10, 12, 13-D_4 acid (13-HODE-D_4) were obtained from Cayman Chemical Company (Ann Arbor, MI). Other materials were of the highest commercial grade available. Cells exposed to NiO nanoparticles were collected by 0.25% trypsinization, washed once with PBS, and resuspended in 0.5 m*l* of PBS. Methanol (0.5 m*l*) including 5 μl (50 ng) of each internal standard was added to 0.5 m*l* of cell suspension. To reduce the concentration of hydroperoxides and ketones in the solution, 20 mg of sodium borohydride was added and kept under an atmosphere of nitrogen for 5 min. The reduced sample was mixed with 1 M potassium hydroxide in methanol (0.5 m*l*) under a nitrogen atmosphere and incubated for 30 min in darkness at 40°C on a shaker. After the sample was chilled on ice, the sample was neutralized with 2 m*l* of 10% acetic acid. Five milliliters of chloroform–acetic ether (4:1) were added to the neutralized sample and vortex-mixed for 30 s. The sample was centrifuged at 3,000 × g for 10 min at 4°C, and the upper layer and proteins were removed by aspiration. After the extract was dried by a rotary evaporator, it was re-solved in 300 μl of methanol–water (70:30) and subjected to liquid chromatography using a LC-20AB system (Shimadzu Corporation, Kyoto, Japan) equipped with a quadrupole mass spectrometer (Finnigan TSQ Quantum Discovery Max; Thermo Fisher Scientific Inc., Waltham, MA). A Hypersil Gold column (25003-102130, 100 mm × 2.1 mm, 3-μm particle size, Thermo Scientific) was used.

Determination of glutathione (GSH) content

Intracellular GSH content was determined enzymatically using 5,5'-dithiobis-(2-nitrobenzoic acid) (DTNB), according to the method of Anderson[40]. Treated cells (1.7×10^5 cells) were harvested by trypsinization, washed with cold PBS and resuspended in 190 μl of PBS. An equal volume of ice-cold 10% trichloroacetic acid (TCA) was added to 150 μl of the cell suspension; then, cell samples were vortex-mixed for 1 minute and centrifuged at 1,000 × g for 15 min. The treated supernatant was mixed with 0.2 M phosphate buffer (pH 7.5) containing 5 mM EDTA, 0.2 mM NADPH, and 1.0 U/m*l* GSH reductase, and maintained at 37°C. Absorbance at 412 nm was measured following the addition of 1.0 mM DTNB. The GSH content was calculated using reduced GSH (Nacalai Tesque, Kyoto, Japan) as the standard.

Real-time polymerase chain reaction

The expression of target genes was determined using Real Time-PCR. Total RNA was isolated from cells using the RNeasy mini kit (Qiagen GmbH, Hilden, Germany). cDNA synthesis was carried out with a High Capacity cDNA Reverse Transcription kit (Applied Biosystems, Carlsbad, CA). Real Time-PCR was conducted using a Step One Real Time-PCR system (Applied Biosystems), and PCR amplification was detected with power SYBR Green PCR master mix (Applied Biosystems). Human ribosomal protein L32 (RiboL32) was used as an endogenous control. The primers for amplification were: RiboL32, 5'-GTA ACT GGC GGA AAC CCA-3' (forward), 5'-AGA TCT GGC CCT TGA ATC TTC-3' (reverse); HO-1, 5'-GGG TGA TAG AAG AGG CCA AGA CT-3' (forward), 5'-AGC TCC TGC AAC TCC TCA AAG A-3' (reverse); SP-D, 5'- ACA CAG GCT GGT GGA CAG TTG-3' (forward), 5'-TTG CAA GGC GGC ATT CTC-3' (reverse).

Animals and intratracheal instillation

All animal experiments were approved by the Institutional Animal Care and Use Committee of National Institute of Advanced Industrial Science and Technology (AIST).

Eight-week-old male Wistar rats were obtained from CLEA Japan, Incorporated (Tokyo, Japan). Rats were fed a standard diet and they were allowed to acclimatize to the environment for one week before experimentation.

A NiO dispersion at a concentration of 0.2 mg per 0.4 m*l* was administered to rats by a single intratracheal instillation. Control rats were given only 0.4 m*l* of distilled water. Each group included at least four rats. At 1, 4, 24 and 72 h and 1 wk after exposure, rats were anesthetized by intraperitoneal injection of pentobarbital sodium (Nembutal: Dainippon Sumitomo Pharma Co., Ltd., Osaka, Japan). At autopsy, blood was taken from the abdominal aorta; then, the lung was perfused with saline. Bronchoalveolar lavage fluid (BALF) was recovered by administering 5 m*l* of saline into the right lung while clamping the left main bronchus. The injection and recovery of saline was repeated thrice, and BALF of a total volume of 15 m*l* was collected. BALF was centrifuged at 1,500 rpm for 10 min to remove cell debris. The supernatant was collected and used for the measurement of markers.

Measurement of biomarkers in BALF

Analyses of tHODE were performed using liquid chromatography coupled to quadrupole mass spectrometry (LC–MS/MS). Methanol (0.5 m*l*) including 5 μl (50 ng) of each internal standard was added to 0.5 m*l* of BALF. The following assays were carried out as well as measurement of the cultured cells.

The concentration of lactate dehydrogenase (LDH) in BALF was measured with a tetrazolium salt using a Cytotoxicity Detection Kit^{PLUS} (LDH) (Roche Diagnostics GmbH, Mannheim, Germany) according to the manufacturer's instructions. The amount of formazan salt formed was measured at 492 nm using a Multiskan Ascent plate reader (Thermo Labsystems, Helsinki, Finland).

LDH activity was estimated by a standard curve obtained from known concentrations of LDH from porcine heart (Serva Electrophoresis GmbH, Heidelberg, Germany). HO-1 concentration in BALF was detected by enzyme-linked immunosorbent assay (ELISA) using a Rat Heme Oxygenase-1 EIA Kit (Takara Bio Incorporated, Otsu, Japan). The concentration of surfactant-associated protein D (SP-D) in BALF was measured using an ELISA kit for rat SP-D (Uscn Life Science Incorporated, Wuhan, China).

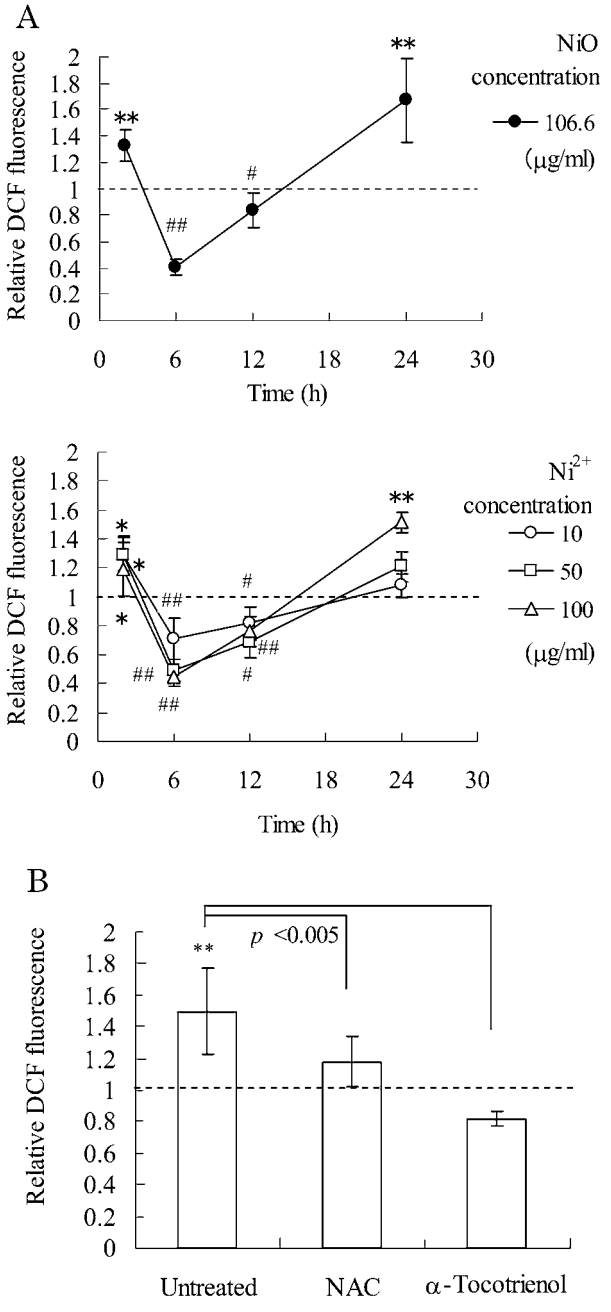

Statistical analysis

Data are presented as means ± S.D. of at least three separate experiments. Statistical analyses were performed using the unpaired *t*-test or analysis of variance (ANOVA) using the Dunnett or Tukey tests for multiple comparisons. The calculation method used is described in each figure legend.

Results

Cellular responses induced by NiO nanoparticles

The NiO nanoparticles dispersion medium prepared for *in vitro* experiments included secondary particles whose average sizes, estimated by distributions based on light intensity and number, were approximately 130–180 nm and 70–110 nm, respectively.

The dispersion had a monomodal size distribution. The light scattering intensity of the NiO dispersion medium did not change over the experimental period, so the NiO dispersion medium used in the *in vitro* experiments was stable. The dispersed NiO medium contained 106.6 μg/m*l* of NiO and 45.8 μg/m*l* of ionized Ni^{2+}.

Human lung carcinoma A549 cells were incubated in the NiO dispersion medium, and at 2, 6, 12 and 24 h of incubation, the intracellular ROS level was measured (Fig. 1). The fluorescent intensities of cells not exposed to NiO and incubated for 2, 6, 12 and 24 h were 21.8, 20.9, 16.1 and 20.1, respectively, without significant differences. Compared with unexposed cells, the intracellular ROS level of NiO-exposed cells was significantly increased 2 h after exposure. Subsequently, the intracellular ROS level had decreased at 6 h of exposure. The intracellular ROS level of cells at 6 h of exposure to NiO nanoparticles was significantly lower than that of unexposed cells. Compared with 6 h of exposure, the intracellular ROS level of cells

Fig. 1. Intracellular ROS levels of cells exposed to NiO nanoparticles. (A) A549 cells were incubated in the NiO–DMEM–FBS dispersion. Intracellular ROS levels were measured by the DCFH method after exposures of 2, 6, 12 and 24 h. Intracellular ROS levels are shown relative to the values of unexposed cells. The concentration of extracellular Ni^{2+} was 50 μg/m*l*. The concentration of NiO particles was 106.6 μg/m*l*. The intracellular ROS levels of cells exposed to $NiCl_2$ solution were also measured as a control for extracellular Ni^{2+}. (B) Effects of anti-oxidants on intracellular ROS levels. The A549 cells were pre-treated with 5 μM α-tocotrienol (α-Toc-3) and 2 mM of NAC for 24 h. Then the cells were exposed to the NiO DMEM-FBS dispersion for 24 h. Significant differences are shown in the figure (vs. unexposed cells, ANOVA, Dunnett). $^{\#}$ indicates significantly lower than unexposed cells. * indicates significantly higher than unexposed cells. **, $^{\#\#}$: $p<0.01$, *, $^{\#}$: $p<0.05$.

exposed to NiO nanoparticles had increased again at 12 h of exposure. The intracellular ROS level of cells exposed to NiO nanoparticles at 24 h of exposure was significantly higher than that of unexposed cells. The intracellular ROS level of cells exposed to NiO nanoparticles showed a decrease from 2 to 6 h of exposure, followed by an increase from 6 to 24 h of exposure. At 24 h of NiO exposure, the intracellular ROS level of cells exposed to NiO nanoparticles was 1.5 times higher than that of unexposed cells.

The influence of extracellular Ni^{2+} on intracellular ROS level was also examined (Fig. 1A). The intracellular ROS level of $NiCl_2$-exposed cells showed a similar dynamic state to NiO-exposed cells. The influence of $NiCl_2$ on cells was weaker than that of NiO nanoparticles. Even when the extracellular Ni^{2+} concentration was similar (~50 μg/m*l*), the intracellular ROS level did not significantly increase in cells exposed to $NiCl_2$ for 24 h. The decrease in the intracellular ROS level at 6 h of exposure was dependent upon the extracellular Ni^{2+} concentration.

The increase in intracellular ROS levels was reduced by pre-treating the cells with antioxidants, 5 μM of α-tocotrienol and 2 mM of NAC (Fig. 1B). NAC is readily taken up by cells and subsequently acts as a source of cellular GSH. α-Tocotrienol acts as lipophilic radical scavenger. Treatment with α-tocotrienol, which has higher cellular uptake efficiency[41] than α-tocopherol, suppressed the raised intracellular ROS levels induced by NiO nanoparticles. This result supports the hypothesis that increases in intracellular ROS levels are caused by cellular uptake of NiO nanoparticles.

Intracellular lipid peroxidation levels in cells exposed to NiO or $NiCl_2$ were measured (Fig. 2A). The intracellular lipid peroxidation level followed a similar dynamic to the intracellular ROS level, i.e., the intracellular lipid peroxidation level increased, subsequently decreased, and then increased again. The oxidation products of fatty acids were examined. The oxidation product of linoleic acid, tHODE, was increased in cultured cells by exposure to NiO for 24 h (Fig. 2B). Exposure to $NiCl_2$ did not induce an increase in the tHODE level of cells.

The intracellular level of GSH was reduced by exposure to NiO nanoparticles and $NiCl_2$ for 24 h (Fig. 3A). The gene expression level of HO-1 (which has antioxidative activity) was increased significantly at 6 and 24 h of exposure to NiO and $NiCl_2$ (Fig. 3B). The gene expression level of SP-D was increased at 24 h of exposure.

These results suggest that oxidative stress is induced by NiO nanoparticles and the antioxidant systems of cells are activated by this oxidative stress.

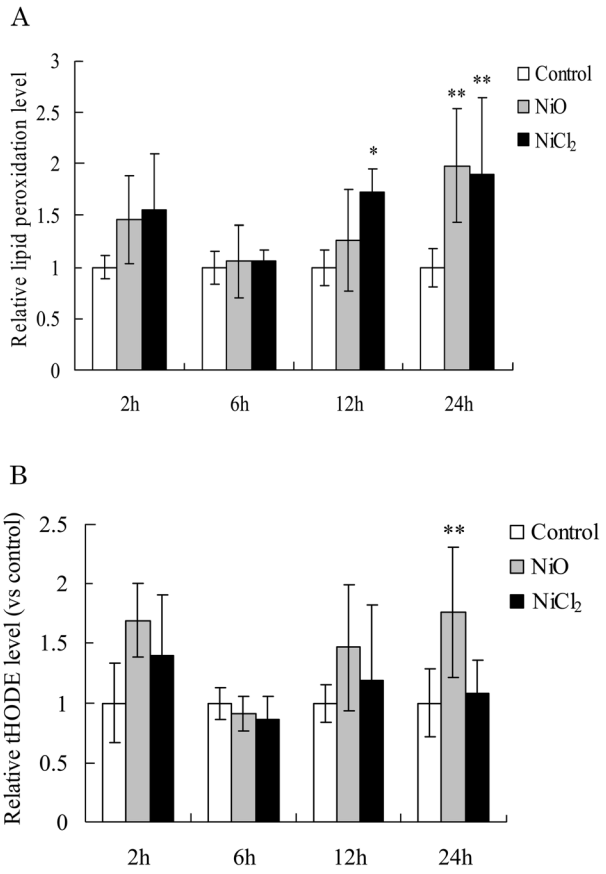

Fig. 2. The lipid peroxidation of cells exposed to NiO nanoparticles. (A) A549 cells were incubated in the NiO-DMEM-FBS dispersion. Intracellular lipid peroxidation levels were measured by the DPPP method after exposures of 2, 6, 12 and 24 h. Lipid peroxidation levels are shown relative to the values of unexposed cells. (B) tHODE levels in cells exposed to NiO nanoparticles. A549 cells were incubated in the NiO-DMEM-FBS dispersion. Concentrations of tHODE were measured by LC-MS/MS after exposures of 2, 6, 12 and 24 h. Levels of tHODE are shown relative to the values of unexposed cells. The concentration of extracellular Ni^{2+} was 50 μg/m*l*. The concentration of NiO particles was 106.6 μg/m*l*. tHODE levels of cells exposed to $NiCl_2$ solution were measured as a control for extracellular Ni^{2+}. Significant differences are shown in the figure (vs. unexposed cells, ANOVA, Dunnett). "*" indicates significantly higher than unexposed cells (**: $p<0.01$, *: $p<0.05$).

Analysis of BALF obtained after the intratracheal instillation of NiO nanoparticles

Next, we examined the biological responses induced by NiO nanoparticles *in vivo*. A dispersion of NiO in water was prepared for the *in vivo* experiments. The size of the NiO particles was measured by the DLS technique, and the mean particle sizes, estimated by the distributions based on light intensity and number, were 39.05 nm and 27.11 nm, respectively. The NiO dispersion was instilled into the trachea of rats at 200 μg per rat. The maximum

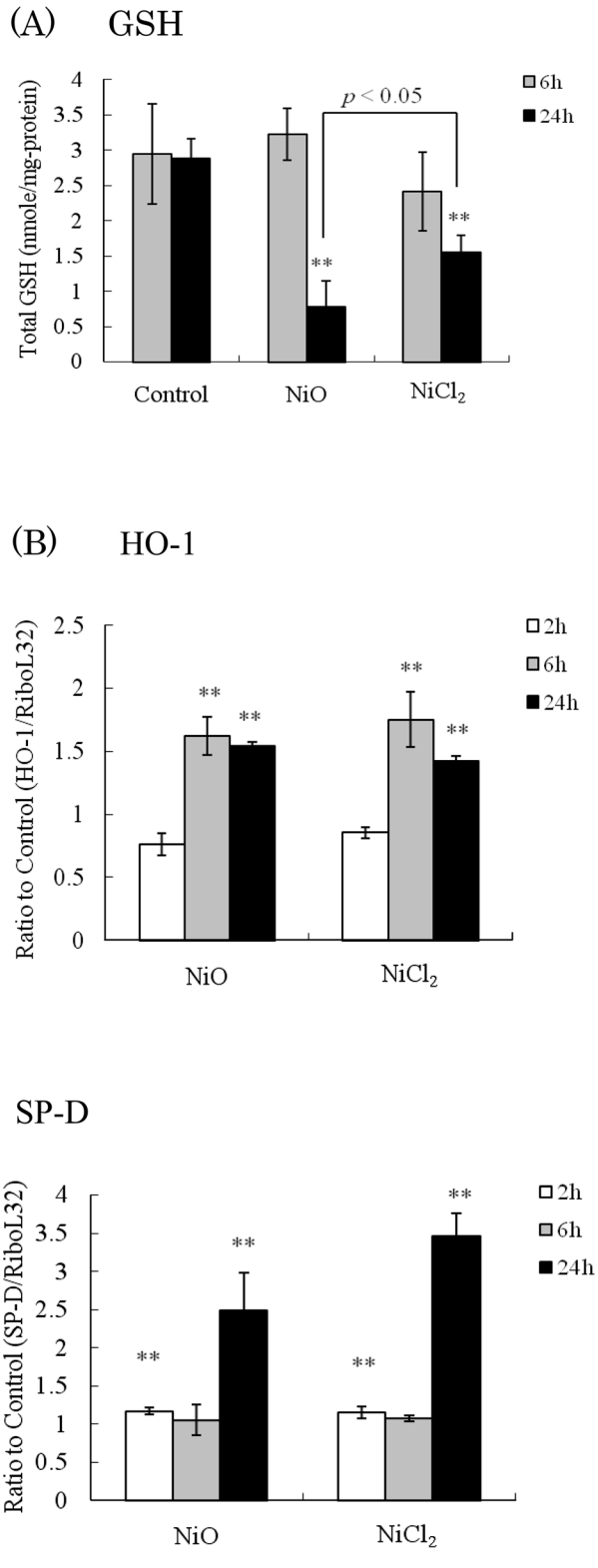

concentration of NiO in the lung was 500 μg/m*l*. BALF was collected at 1, 4, 24, 72 h (3 days) and 168 h (7 days) after intratracheal instillation. Compared with control animals, LDH activity in the BALF was significantly increased at 3 and 7 days after instillation (Fig. 4). Although LDH activity in the BALF obtained from NiO-instilled animals tended to increase 24 h after instillation, a significant difference was not observed. The relative levels of tHODE in BALF were significantly increased compared with the control 24 h after instillation of NiO nanoparticles (Fig. 5). In particular, the concentration of tHODE in BALF was higher than the control from 24 h to 3 days after instillation. The time-dependent change of the tHODE level induced by NiO exposure in BALF showed a similar tendency to that observed *in vitro*.

The antioxidant responses of NiO-instilled rats were also examined. The concentration of HO-1 protein in BALF increased 24 h and 3 days after instillation. The concentration of SP-D in BALF increased 3 days and 7 days after instillation (Fig. 6). HO-1 is a well-known oxidative stress response enzyme, and HO-1 and SP-D have antioxidant properties[42, 43]. These results suggest that intratracheal instillation of NiO nanoparticles induced oxidative stress and subsequent lung injury, and that an antioxidant defense system was simultaneously activated.

The results obtained in the *in vivo* experiments conformed to the results obtained in the *in vitro* experiments.

Discussion

It was reported that intratracheal instillation of NiO

Fig. 3. Cellular responses related to antioxidation induced by exposure to NiO nanoparticles. (A) Intracellular glutathione levels of cells exposed to NiO nanoparticles. A549 cells were incubated in the NiO-DMEM-FBS dispersion. Intracellular GSH levels were measured after 6 and 24 h of exposure. The concentration of extracellular Ni^{2+} was 50 μg/m*l*. The concentration of NiO particles was 106.6 μg/m*l*. GSH levels of cells exposed to $NiCl_2$ solution were exposed cells was measured as a control for extracellular Ni^{2+}. (B) Gene expression of HO-1 and SP-D in cells exposed to NiO nanoparticles. A549 cells were incubated in the NiO-DMEM-FBS dispersion. Gene expressions of HO-1 and SP-D were measured by real-time PCR after exposures of 2, 6 and 24 h. The concentration of extracellular Ni^{2+} was 50 μg/m*l*. The concentration of NiO particles was 106.6 μg/m*l*. The plotted values are relative values: HO-1/RiboL32 and SP-D/RiboL32 of the unexposed cells are 1.0, respectively. Significant differences are shown in the figure (vs. unexposed cells, ANOVA, Dunnett). * indicates significantly higher than unexposed cells (**: p<0.01).

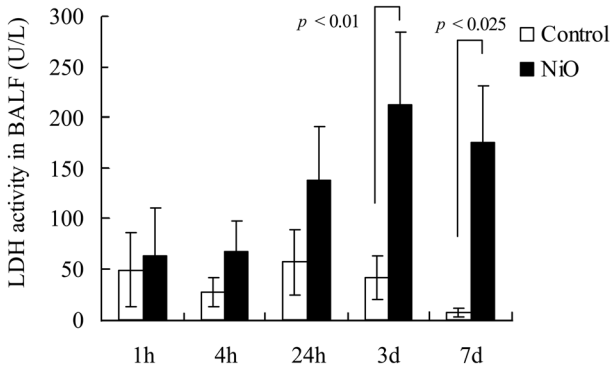

Fig. 4. LDH activity in BALF after intratracheal instillation of NiO nanoparticles into rats. BALF was collected 1 h, 4 h, 24 h, 3 days and 7 days after instillation of 0.4 m*l* of the dispersion containing 200 μg of NiO nanoparticles. LDH activity was then measured. The control group was given only 0.4 m*l*/rat of distilled water. Significant differences between NiO-instilled rats and the control rats are indicated in the figure (unpaired *t*-test).

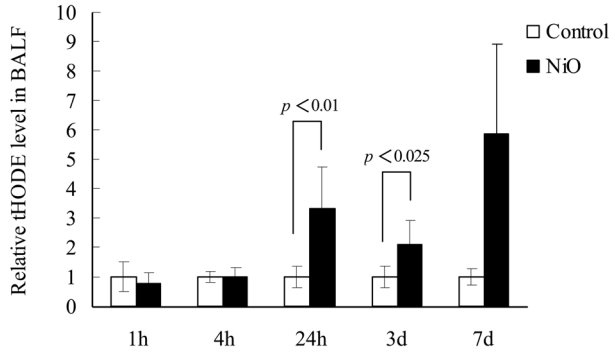

Fig. 5. Lipid peroxidation level in BALF after intratracheal instillation of NiO nanoparticles into rats. BALF was collected 1 h, 4 h, 24 h, 3 days and 7 days after instillation of 0.4 m*l* of the dispersion containing 200 μg of NiO nanoparticles. The concentration of tHODE was then measured. The control group was given only 0.4 m*l*/rat of distilled water. Levels of tHODE are shown relative to the control. Significant differences between the NiO-instilled rats and control rats are indicated in the figure (unpaired *t*-test).

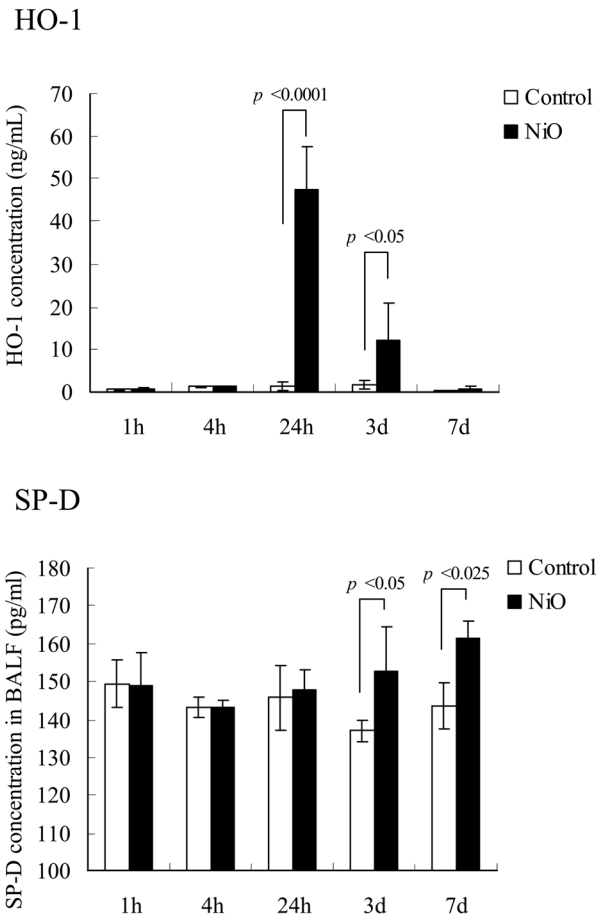

Fig. 6. Concentrations of HO-1 and SP-D in BALF after intratracheal instillation of NiO nanoparticles into rats. BALF was collected 1 h, 4 h, 24 h, 3 days and 7 days after instillation of 0.4 m*l* of the dispersion containing 200 μg of NiO nanoparticles. The concentrations of HO-1 and SP-D were then measured. The control group was given only 0.4 m*l*/rat of distilled water. Significant differences between the NiO-instilled rats and control rats are indicated in the figure (unpaired *t*-test).

nanoparticles induced expression of inflammation-related cytokines[44]. In the present study, the relationship between the oxidative stress induced by NiO particles *in vitro* and *in vivo* was examined.

Exposure of NiO nanoparticles induced oxidative stress and activation of antioxidant systems in cultured cells *in vitro* and rat lungs *in vivo*. In cultured cells, DCF fluorescence, DPPP oxide fluorescence and tHODE levels were significantly increased by exposed to NiO nanoparticles. DPPP oxide fluorescence and tHODE levels indicate lipid peroxide and oxidized linoleic acid levels in the cell, respectively. DPPP has high lipophilicity, and thus, selectively detects lipid peroxide at the biomembrane[45]. These results indicate that NiO nanoparticles induce intracellular ROS generation at the cytosol and then lipid oxidization at the biomembrane. It has been suggested that Ni^{2+} generates ROS by a Fenton-like reaction[46]. If this were the case, then the following chain of events would occur: NiO releases Ni^{2+} and Ni^{2+} generates ROS; subsequently ROS oxidize biomolecules such as lipids. On the other hand, oxidative stresses drove antioxidation systems. The HO-1 gene expression level increased at 24 h after intratracheal instillation of NiO,

and then decreased at 3 days and 1 wk after instillation. Compared with HO-1 expression, the SP-D gene expression level increased at 3 days and 1 wk after NiO instillation. HO-1 is known as a major stress-response protein, and its gene expression is induced by various stresses. Oxidative stress induces gene expression of HO-1 via Nrf2[17]. HO-1 catalyzes the degradation of heme, producing biliverdin, iron, and carbon monoxide. Biliverdin and bilirubin (the reduced product of biliverdin) have strong antioxidant activities[47]. Also, it is known that SP-D has an antioxidative activity[43]. We hypothesize that two steps are involved in the oxidative stress loading mechanism induced by NiO nanoparticles. First, primary oxidative stress occurs, 24 h after instillation, due to the direct effect of NiO nanoparticles, released Ni^{2+} and subsequent generation of ROS by Fenton-like reaction. In this first phase, the induced expression of HO-1 removes the oxidative stress, resulting in temporal reduction of oxidative stress and avoidance of lung injury, indicated by LDH release. The secondary oxidative stress occurred at 3 days and later after instillation of NiO nanoparticles and is caused by indirect effects. This later event is induced by secretion of proinflammatory cytokines and subsequent macrophage accumulation. Actually, at 3 days after intratracheal instillation of NiO nanoparticles, the secretion of inflammatory cytokines, and infiltration of alveolar macrophages and neutrophils were observed[44]. We consider that HO-1 expression was reduced with the weakening of the primary oxidative stress. In contrast, SP-D was induced by a continuous oxidative stress which could not be removed from the antioxidation system in the first phase. According to the results of our *in vitro* experiments, SP-D gene expression occured later than HO-1 gene expression. After 24 h exposure to NiO nanoparticles, the tHODE level and HO-1 gene expression increased in both the *in vitro* and *in vivo* experiments. Increase of the intracellular ROS level at 2 h of exposure was caused by NiO nanoparticles or released Ni^{2+}. The first antioxidation system, HO-1, had not been activated by 2 h of exposure as shown in Fig. 3. After 6 h exposure, HO-1 gene expression had increased and cells were supplied with sufficient amounts of GSH. Therefore, intracellular ROS decreased at 6 h exposure. HO-1 gene expression did not decrease in cultured cells because NiO particles or Ni^{2+} cannot be cleared from an *in vitro* system, whereas the number of antioxidant molecules, e.g. GSH, HO-1 and SP-D, is limited *in vitro*. As fresh antioxidants are not supplied to culture media and cells, the continuous oxidative stress induced by nickel compounds will eventually overcome the cellular defense system *in vitro*. Continuous ROS generation will lead to failure in the cellular antioxidant system. For example, GSH depletion (Fig. 3(A)), would lead to an increase in the intracellular ROS level. Although "secondary oxidative stress" does not occur in cultured cells without macrophages, it would be predictable by "primary oxidative stress."

Exposure to NiO nanoparticles induced oxidative stresses *in vivo* and *in vitro*. As a result, the oxidation products of biological molecules such as lipid peroxide were produced. tHODE levels in cells and BALF were increased by exposure to NiO nanoparticles. Linoleic acid (which is the starting material of tHODE) is one of major unsaturated fatty acids in the rat lung[48] which is comprised of approximately 20% of linoleic acid. Moreover, since tHODE is water soluble, produced tHODE easily dissolves in BALF. Since antioxidative systems such as GSH, HO-1 and SP-D were activated, it can be said that the induction of oxidative stress is the result of an acute reaction. In the present study, we revealed the acute responses are induced by NiO nanoparticles in the lung. The acute toxicity induced by NiO nanoparticles was reflected in *in vitro* experiments to a certain degree.

In this study, the secondary particle sizes were different in the *in vitro* and the *in vivo* dispersions. For the *in vitro* examinations, it was necessary to disperse NiO nanoparticles in the culture medium. Cell culture media include high concentrations of proteins and salts. Therefore, NiO nanoparticles form large aggregates with proteins and salts in the medium. On the other hand, the NiO dispersion used for the *in vivo* experiments did not include proteins or salts. The secondary particle size of the dispersed NiO medium used for the *in vitro* experiments reflected the actual cell exposure size. However, the secondary particle size of the NiO water dispersion used for the *in vivo* experiments did not reflect the actual exposure size. After intratracheal instillation, NiO nanoparticles may have adsorbed proteins or the surfactant which would have led to changes in secondary particle size. Although the measurement of the secondary particle size in the lung by DLS is technically impossible, we previously reported, in a TiO_2 study, that there were no differences in the cellular influences induced by secondary particle sizes in the range of particles (both *in vitro* and *in vivo*) used in this study (40–180 nm as secondary particle size)[36].

Although *in vivo* experiments provide critical information about biological influences for risk assessment, *in vivo* systems are very complicated. Accordingly, the mechanistic information obtained from *in vivo* experiments is usually insufficient. *In vitro* experiments are simpler and can provide mechanistic information about biological influences rapidly and at low cost. However *in vitro* examinations often lack correlation with physiological systems. In the present study, we demonstrated that the acute toxicity induced by metal oxide nanoparticles could be evaluated by a combination of *in vivo* and *in vitro* experiments. Although the prediction of long-term toxicity such as carcinogenicity by *in vitro* examination is very difficult, it is effective for the study of the acute toxicity of metal oxide particles.

Acknowledgments: This work was funded by a grant from the New Energy and Industrial Technology Development Organization (NEDO) entitled "Evaluating risks associated with manufactured nanomaterials (P06041)".

References

1) Dunnick JK, Benson JM, Hobbs CH, Hahn FF, Cheng YS, Eidson AF. Comparative toxicity of nickel oxide, nickel sulfate hexahydrate, and nickel subsulfide after 12 days of inhalation exposure to F344/N rats and B6C3F1 mice. Toxicology 1988; 50: 145–56.
2) Benson JM, Henderson RF, McClellan RO. Comparative cytotoxicity of four nickel compounds to canine and rodent alveolar macrophages *in vitro*. J Toxicol Environ Health 1986; 19: 105–10.
3) Oller AR, Costa M, Oberdörster G. Carcinogenicity assessment of selected nickel compounds. Toxicol Appl Pharmacol 1997; 143: 152–66.
4) Horie M, Nishio K, Fujita K, et al. Ultrafine NiO particles induce cytotoxicity *in vitro* by cellular uptake and subsequent Ni(II) release. Chem Res Toxicol 2009; 22: 1415–26.
5) Veranth JM, Kaser EG, Veranth MM, Koch M, Yost GS. Cytokine responses of human lung cells (BEAS-2B) treated with micron-sized and nanoparticles of metal oxides compared to soil dusts. Part Fibre Toxicol 2007; 4: 2.
6) Huang X, Zhuang Z, Frenkel K, Klein CB, Costa M. The role of nickel and nickel-mediated reactive oxygen species in the mechanism of nickel carcinogenesis. Environ Health Perspect 1994; 102 (Suppl 3): 281–4.
7) Halliwell B. Role of free radicals in the neurodegenerative diseases: therapeutic implications for antioxidant treatment. Drugs Aging 2001; 18: 685–716.
8) Roberts CK, Sindhu KK. Oxidative stress and metabolic syndrome. Life Sci 2009; 84: 705–12.
9) Hussain SP, Harris CC. Molecular epidemiology of human cancer: contribution of mutation spectra studies of tumor suppressor genes. Cancer Res 1998; 58: 4023–37.
10) Toyokuni S. Reactive oxygen species-induced molecular damage and its application in pathology. Pathol Int 1999; 49: 91–102.
11) Toyokuni S, Mori T, Dizdaroglu M. DNA base modifications in renal chromatin of Wistar rats treated with a renal carcinogen, ferric nitrilotriacetate. Int J Cancer 1994; 57: 123–8.
12) Kasai H. Analysis of a form of oxidative DNA damage, 8-hydroxy-2'-deoxyguanosine, as a marker of cellular oxidative stress during carcinogenesis. Mutat Res 1997; 387: 147–63.
13) Kawanishi S, Hiraku Y, Murata M, Oikawa S. The role of metals in site-specific DNA damage with reference to carcinogenesis. Free Radic Biol Med 2002; 32: 822–32.
14) Kawanishi S, Hiraku Y, Oikawa S. Mechanism of guanine-specific DNA damage by oxidative stress and its role in carcinogenesis and aging. Mutat Res 2001; 488: 65–76.
15) Cadet J, Douki T, Gasparutto D, Ravanat JL. Oxidative damage to DNA: formation, measurement and biochemical features. Mutat Res 2003; 531: 5–23.
16) Niki E. Oxidative stress and aging. Intern Med 2000; 39: 324–6.
17) Naito Y, Takagi T, Yoshikawa T. Heme oxygenase-1: a new therapeutic target for inflammatory bowel disease. Aliment Pharmacol Ther 2004; 20 (Suppl 1): 177–84.
18) Ishii T, Itoh K, Takahashi S, et al. Transcription factor Nrf2 coordinately regulates a group of oxidative stress-inducible genes in macrophages. J Biol Chem 2000; 275: 16023–9.
19) Nagatomo H, Morimoto Y, Ogami A, et al. Change of heme oxygenase-1 expression in lung injury induced by chrysotile asbestos *in vivo* and *in vitro*. Inhal Toxicol 2007; 19: 317–23.
20) Nagatomo H, Morimoto Y, Oyabu T, et al. Expression of heme oxygenase-1 in the lungs of rats exposed to crystalline silica. J Occup Health 2006; 48: 124–8.
21) Niki E. Eustress and distress. Nippon Yakurigaku Zasshi 2007; 129: 76–9.
22) Frankel EN. Chemistry of free radical and singlet oxidation of lipids. Prog Lipid Res 1984; 23: 197–221.
23) Ohashi N, Yoshikawa M. Rapid and sensitive quantification of 8-isoprostaglandin F2α in human plasma and urine by liquid chromatography–electrospray ionization mass spectrometry. J Chromatogr B 2000; 746: 17–24.
24) Yoshida Y, Niki E. Detection of lipid peroxidation *in vivo*: total hydroxyoctadecadienoic acid and 7-hydroxycholesterol as oxidative stress marker. Free Radic Res 2004; 38: 787–94.
25) Yoshida Y, Niki E. Bio-markers of lipid peroxidation *in vivo*: hydroxyoctadecadienoic acid and hydroxycholesterol. Biofactors 2006; 27: 195–202.
26) Yoshida Y, Yoshikawa A, Kinumi T, et al. Hydroxyoctadecadienoic acid and oxidatively modified peroxiredoxins in the blood of Alzheimer's disease patients and their potential as biomarkers. Neurobiol Aging 2008; 30: 174–85.
27) Jira W, Spiteller G, Carson W, Schramm A. Strong increase in hydroxy fatty acids derived from linoleic acid in human low density lipoproteins of atherosclerotic patients. Chem Phys Lipids 1998; 91: 1–11.
28) Metzger K, Angres G, Maier H, Lehmann WD. Lipoxygenase products in human saliva: patients with oral cancer compared to controls. Free Radic Biol Med 1995; 18: 185–94.
29) Yoshida Y, Itoh N, Hayakawa M, et al. Lipid peroxidation induced by carbon tetrachloride and its inhibition by antioxidant as evaluated by an oxidative stress marker, HODE. Toxicol Appl Pharmacol 2005; 208: 87–97.
30) Gurr JR, Wang AS, Chen CH, Jan KY. Ultrafine titanium dioxide particles in the absence of photoactivation can induce oxidative damage to human bronchial epithelial cells. Toxicology 2005; 213: 66–73.
31) Nishi K, Morimoto Y, Ogami A, et al. Expression of cytokine-induced neutrophil chemoattractant in rat lungs

by intratracheal instillation of nickel oxide nanoparticles. Inhal Toxicol 2009; 21: 1030–9.
32) Lu S, Duffin R, Poland C, et al. Efficacy of simple short-term in vitro assays for predicting the potential of metal oxide nanoparticles to cause pulmonary inflammation. Environ Health Perspect 2009; 117: 241–7.
33) Ogami A, Morimoto Y, Myojo T, et al. Pathological features of different sizes of nickel oxide following intratracheal instillation in rats. Inhal Toxicol 2009; 21: 812–8.
34) Morimoto Y, Kobayashi N, Shinohara N, Myojo T, Tanaka I, Nakanishi J. Hazard assessments of manufactured nanomaterials. J Occcup Health 2010; 52: 325–34.
35) Fujita K, Morimoto Y, Ogami A, et al. A gene expression profiling approach to study the influence of ultrafine particles on rat lungs. In: Kim JY, Platt U, Gu MB, H. Iwahashi H, editors. Atmospheric and Biological Environmental Monitoring. Dordrecht (Netherlands): Springer-Verlag GmbH; 2009. p. 221–9.
36) Horie M, Nishio K, Fujita K, et al. Cellular responses by stable and uniform ultrafine titanium dioxide particles in culture-medium dispersions when secondary particle size was 100 nm or less. Toxicol In Vitro 2010; 24: 1629–38.
37) Ohno N, Sakai T, Nakabayashi M, Sasaki H. Spectrophotometric determination of trace amounts of nickel using 2-(5-bromo-2-pyridylazo)-5-(N-propyl-N-sulfopropylamino) aniline. Bunseki Kagaku 1990; 39: 399–403.
38) Kato H, Fujita K, Horie M, et al. Dispersion characteristics of various metal oxide secondary nanoparticles in culture medium for *in vitro* toxicology assessment. Toxicol In Vitro 2010; 24: 1009–18.
39) Yoshida Y, Kodai S, Takemura S, Minamiyama Y, Niki E. Simultaneous measurement of F2-isoprostane, hydroxyoctadecadienoic acid, hydroxyeicosatetraenoic acid, and hydroxycholesterols from physiological samples. Anal Chem 2008; 379: 105–15.
40) Anderson ME. Determination of glutathione and glutathione disulfide in biological samples. Methods Enzymol 1985; 113: 548–55.
41) Saito Y, Yoshida Y, Nishio K, Hayakawa M, Niki E. Characterization of cellular uptake and distribution of vitamin E. Ann N Y Acad Sci 2004; 1031: 368–75.
42) Takahashi T, Shimizu H, Morimatsu H, et al. Heme oxygenase-1: a fundamental guardian against oxidative tissue injuries in acute inflammation. Mini Rev Med Chem 2007; 7: 745–53.
43) Bridges JP, Davis HW, Damodarasamy M, et al. Pulmonary surfactant proteins A and D are potent endogenous inhibitors of lipid peroxidation and oxidative cellular injury. J Biol Chem 2000; 275: 38848–55.
44) Morimoto Y, Ogami A, Todoroki M, et al. Expression of inflammation-related cytokines following intratracheal instillation of nickel oxide nanoparticles. Nanotoxicology 2010; 4: 161–76.
45) Okimoto Y, Warabi E, Wada Y, Niki E, Kodama T, Noguchi N. A novel method of following oxidation of low-density lipoprotein using a sensitive fluorescent probe, diphenyl-1-pyrenylphosphine. Free Radic Biol Med 2003; 35: 576–85.
46) Valko M, Rhodes CJ, Moncol J, Izakovic M, Mazur M. Free radicals, metals and antioxidants in oxidative stress-induced cancer. Chem Biol Interact 2006; 160: 1–40.
47) Stocker R, Yamamoto Y, McDonagh AF, Glazer AN, Ames BN. Bilirubin is an antioxidant of possible physiological importance. Science 1987; 235: 1043–6.
48) Fletcher K, Wyatt I. The composition of lung lipids after poisoning with paraquat. Br J Exp Pathol 1970; 51: 604–10.